Design Proposal – Unbalanced Mach-Zehnder Interferometer

Swayam Prakash Sahoo
username: Swayam_PS[1,2]

[1]Institut Interdisciplinaire d'Innovation Technologique (3IT), Université de Sherbrooke, Sherbrooke, QC J1K 0A5, Canada
[2]Ecole Centrale Lyon, INSA Lyon, CNRS, Institut des Nanotechnologies de Lyon (INL), UMR5270, 69130 Ecully, France
*e-mail: swayam.prakash.sahoo@usherbrooke.ca

1 Introduction

This report outlines the design and modeling of the unbalanced Mach-Zehnder Interferometer(hereafter, MZI) performed as a part of the coursework of Silicon Photonics Design, Fabrication, and Data Analysis – a course offered online by the University of British Columbia that shall lead to its fabrication and analysis.
The MZI is a foundational component in photonic integrated circuits (PICs), enabling precise control and modulation of light for applications in telecommunications, sensing, and quantum optics. Integrated onto compact chips, MZIs leverage waveguide-based architectures to achieve high-performance optical signal processing while minimizing footprint and power consumption. It relies on the principle that light traveling through the arms accumulates a phase difference, leading to constructive or destructive interference at the output. The resulting intensity depends on the relative phase shift

2 Waveguide Design

In the design, a cross-section of the following parameters is considered: 220 $nm \times 600\ nm$. The width of 600 nm is to encapsulate all modes and avoid losses at the edges.

2.1 Modeling

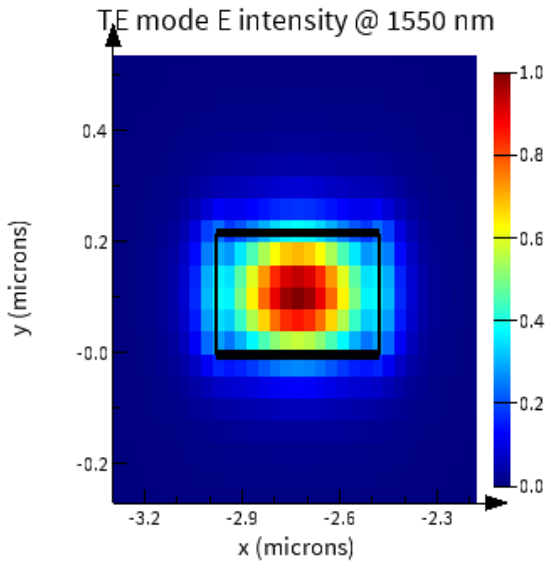

Figure 1. TE mode profile at $\lambda = 1550\ nm$

mode	n_{eff}	wavelength	loss	group index	TE polarization fraction	WG TE/TM fraction
1	2.45	1.55	0.0004	4.21	99	76.06/82.53
2	1.78		0.0003	3.81	4	67.34/88.89

Figure 1 shows that the TE mode is mostly encapulated within the waveguide. The effective index (n_{eff} for the guided TE and TM modes are 2.6 and 1.9 respectively and their polarization fraction is 99% and 4% respectively.

2.2 Incorporating Waveguide dispersion: Effective index and Group index

In addition to the material dispersion, waveguide dispersion needs to be calculated as the geometry of the waveguide dominates the propagative nature of the guided modes. A sweep was performed between $\lambda = 1500\ nm$ and $\lambda = 1600\ nm$ to find the change of real and imaginary part of n_{eff}. This is plotted in Figure 2. The $\frac{dn_{eff}}{d\lambda}$ is negative. Thus pointing out that at lower λ the mode is confined in the waveguide and as wavelength increases, most of the light at larger λ is traveling in the cladding. The low loss of the TE mode characterized by the imaginary part of its n_{eff} is effectively seen.

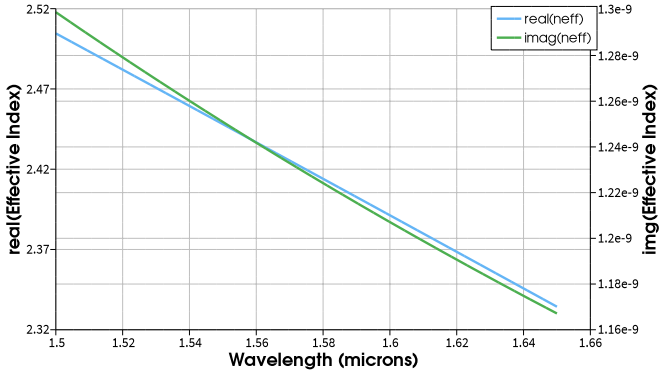

Figure 2. Variation of effective index, n_{eff} vs. λ for TE mode.

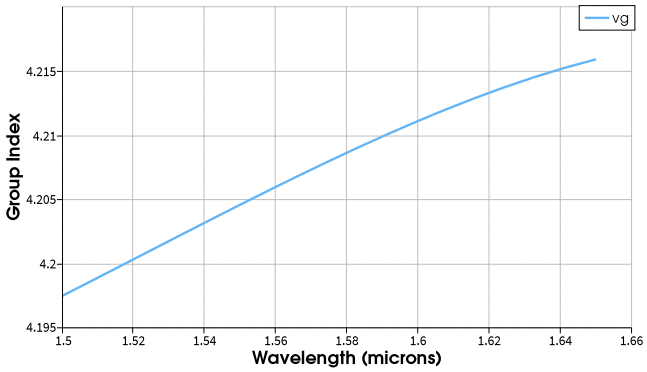

Figure 3. Variation of group index, v_g vs. λ for TE mode.

The next step is fitting the dispersion. Like we did initially to fit the material dispersion, here we shall fit the waveguide dispersion. Mathematically, it can be expressed as[1]:

$$n_{eff}(\lambda) = n_1 + n_2(\lambda - \lambda_0) + n_3(\lambda - \lambda_0)^2 \tag{1}$$

Using this equation, fitting was performed for the real part of n_{eff} displayed in Figure 2. The fitting is shown
At $\lambda_0 = 1550\ nm$, the n_{eff} for the waveguide dimensions of $220\ nm \times 500\ nm$ can be expressed as:

$$n_{eff}(\lambda) = 2.45 - 1.13(\lambda - 1.55) - 0.04(\lambda - 1.55)^2 \tag{2}$$

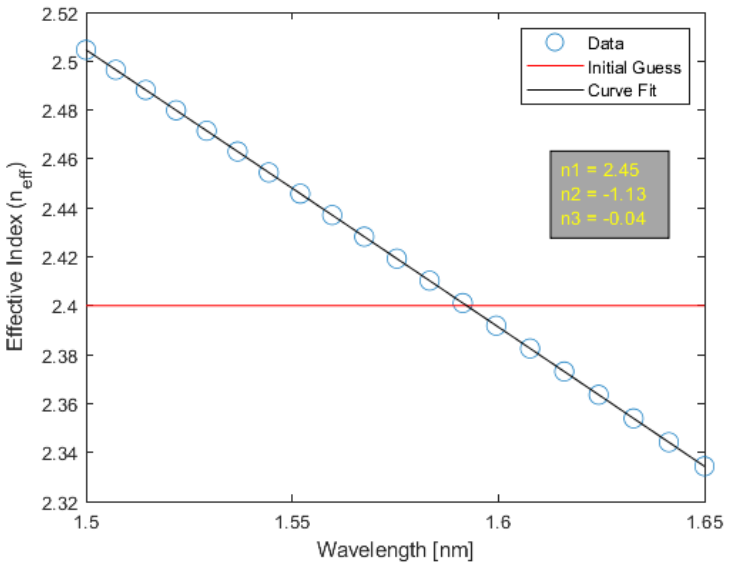

Figure 4. Compact model for the TE mode of a waveguide with dimensions: 220 $nm \times 500\ nm$.

3 MZI

A schematic of MZI implemented using Lumerical INTERCONNECT is shown in Figure 5. Each component is discussed in the subsequent sections.

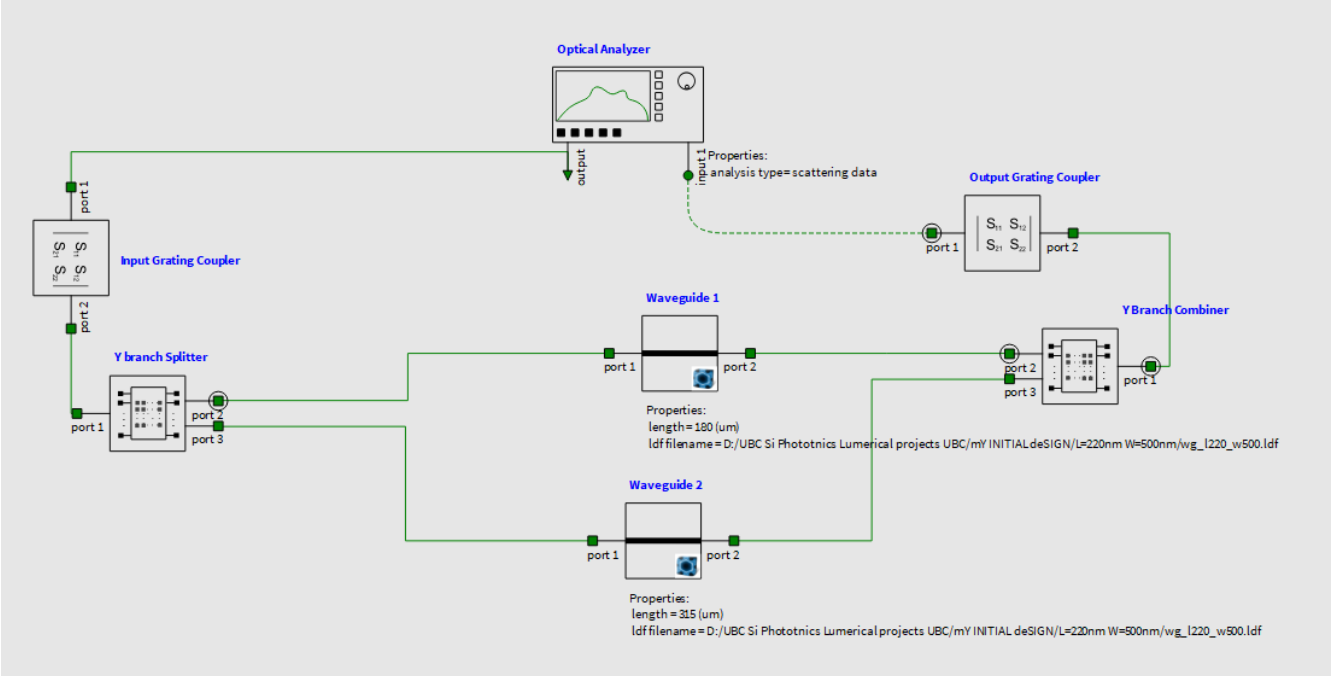

Figure 5. Schematic of MZI with grating couplers and analyzers implemented using Lumerical INTERCONNECT.

3.1 Impact of ΔL on T_{MZI-dB}

The next is to use this waveguide as a phase shifter in an MZI to modulate the output. An MZI will have two grating couples: one at the input and the other at the output. A Y-branch splitter diverging into two unequal waveguides acting as phase shifters.

At the other side of the waveguide is a Y-branch combiner that connects to the output grating coupler. The losses and behaviour of each component need to be modeled.

The transfer function of MZI is:

$$T_{MZI}(\lambda) = \frac{1}{4}\left(1 + e^{-i\beta(\lambda)\Delta L}\right) \tag{3}$$

and in decibels(dB):

$$T_{MZI-dB}(\lambda) = 10\log_{10}[T_{MZI}(\lambda)] \tag{4}$$

Thus, in the path difference, width of both arms, w_1 and w_2 are the kept equal(500 nm) so that β remains quasi-constant ($\Delta\beta = \frac{2\pi n_1}{\lambda} - \frac{2\pi n_2}{\lambda} = 0$) across both arms(theoretically) and only difference in their lengths, $L_2 - L_1 = \Delta L$ is to be considered for generating path difference and interference effects. L_1 is chosen as $L_1 = 180\ \mu m$ and L_2 is varied at $\frac{L_1}{4}$. The plot is shown in Figure 6. The variation of transmission with ΔL is slower when L_1 is longer. The values of transmission for $L_1 = 80\ \mu m$ are shown in Figure 7.

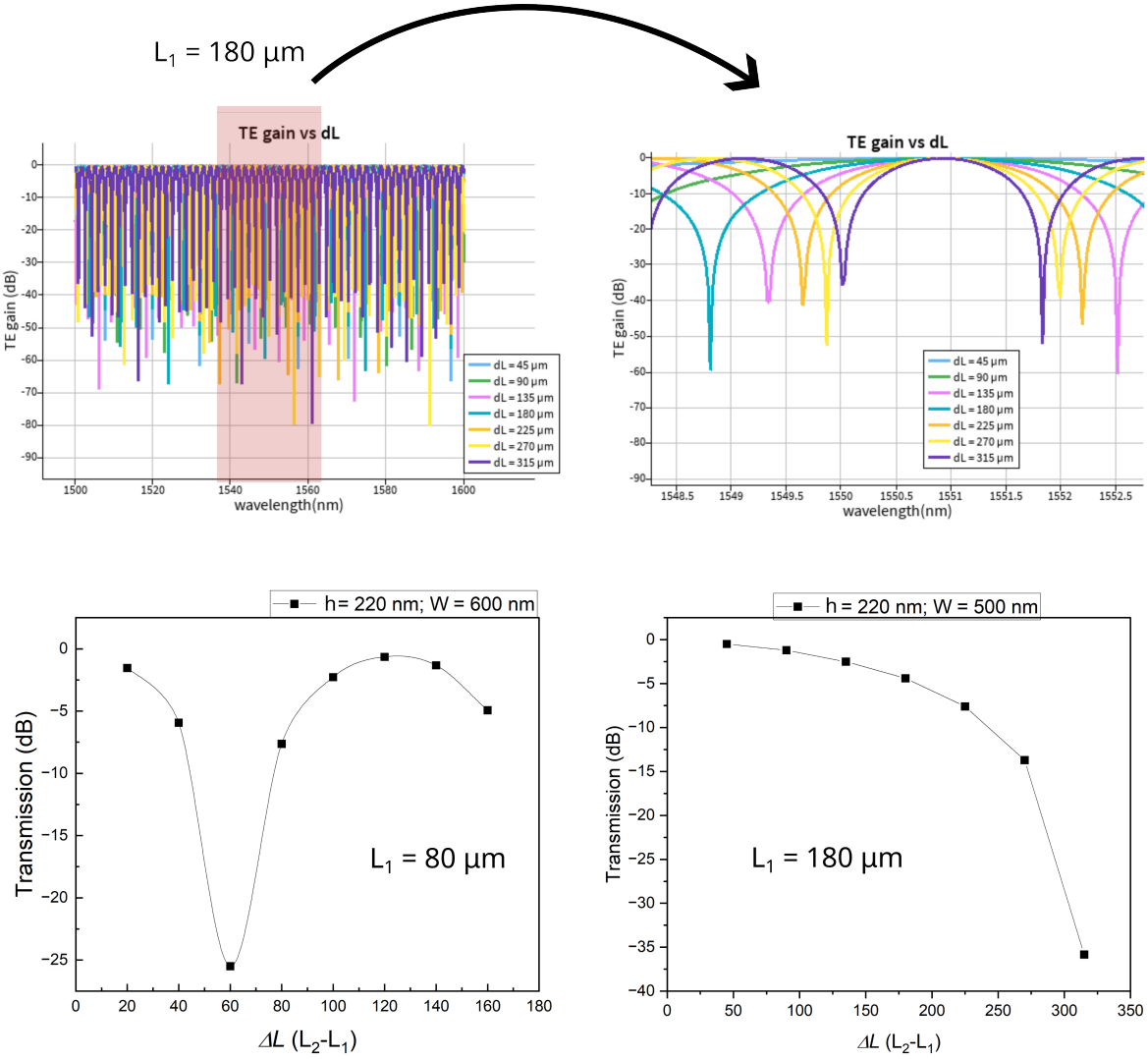

Figure 6. Analytical solutions of Transfer function of TE mode MZI for different ΔL values of $L_1 = 180\ \mu m$. Zoomed-in image shows the Transmission change at $\lambda = 1550\ nm$. which is plotted for various ΔL. Comparison of the variation of transmission for different start values of L_1.

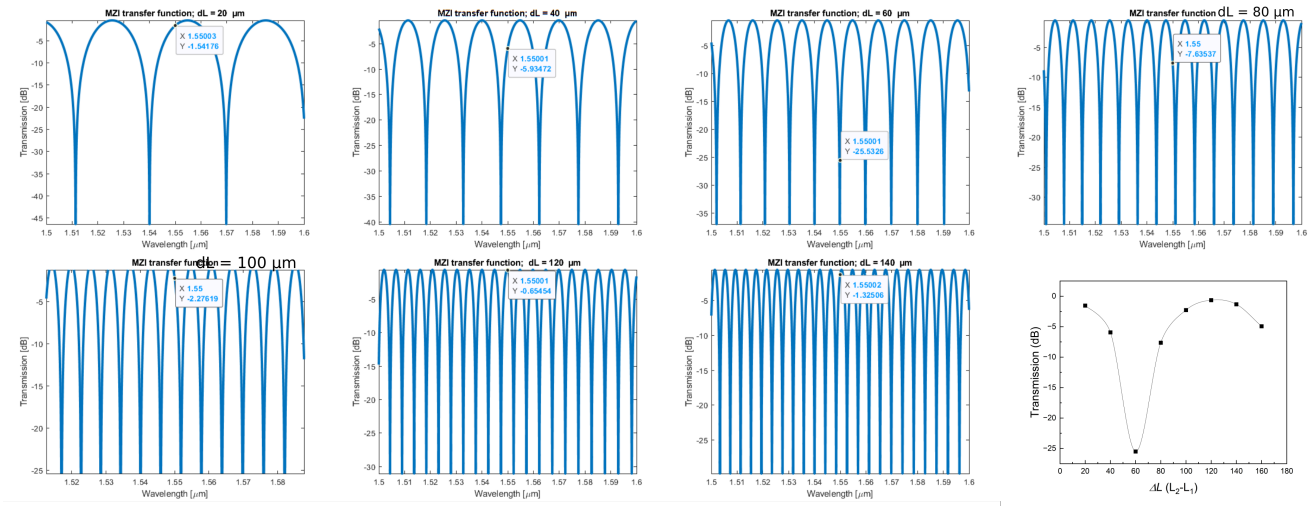

Figure 7. Analytical solutions of Transfer function of TE mode MZI for different ΔL values of $L_1 = 80\ \mu m$. Values are at $\lambda = 1550\ nm$.

3.2 Insertion losses of Grating Couplers

To perform this analysis, we connect the grating couplers to the analyzers and check their inherent insertion losses, otherwise known as their transfer function. The combined insertion loss is $\approx 5.1\ dB$ at $\lambda = 1550\ nm$. This is shown in Figure 8. Figure 9 shows the changes in Transfer function (TE gain) after incorporating the insertion losses of grating couplers.

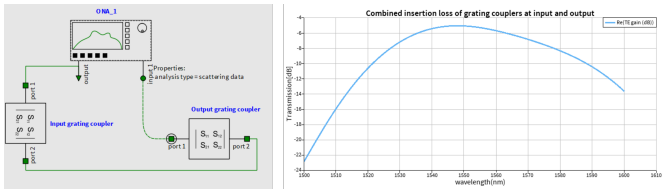

Figure 8. Combined Insertion losses of Grating couplers at input and output.

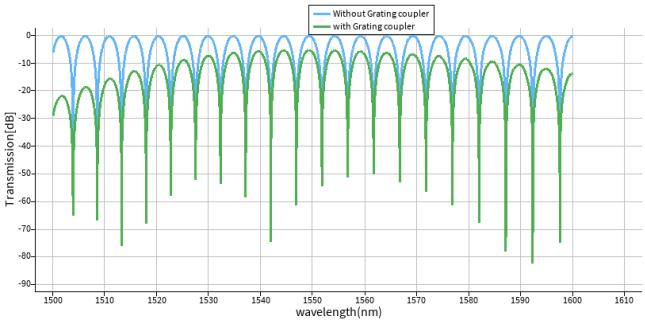

Figure 9. Influence of the insertion losses of Grating couplers on MZI transfer function. The data is presented for $L_1 = 80\ \mu m$;$L_2 = 200\ \mu m$; $\Delta L = 120\ \mu m$.

3.3 Insertion loss of Y-branch

The insertion loss of the simulated Y-branch with s-parameters is shown in Figure 10 where the losses are a function of λ.

3.4 MZI modeling

The MZI circuit shown in Figure 5 will now be modeled taking into account the losses from various components mentioned above. Now, we introduce different ΔL values for $L_1 = 180\ \mu m$ and verify the Transmission and TE gain. The values of

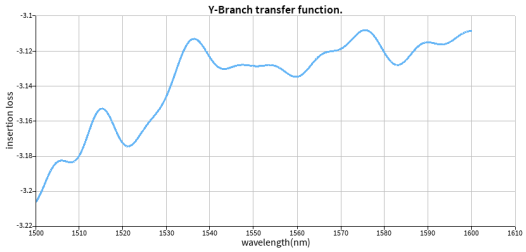

Figure 10. Insertion loss of Y-branch simulated with real data.

ΔL chosen are 568 μm, 225 μm and 100 μm. The data is shown in Figure 11. In the magnified images, it is seen that the transmission is varied for different ΔL.

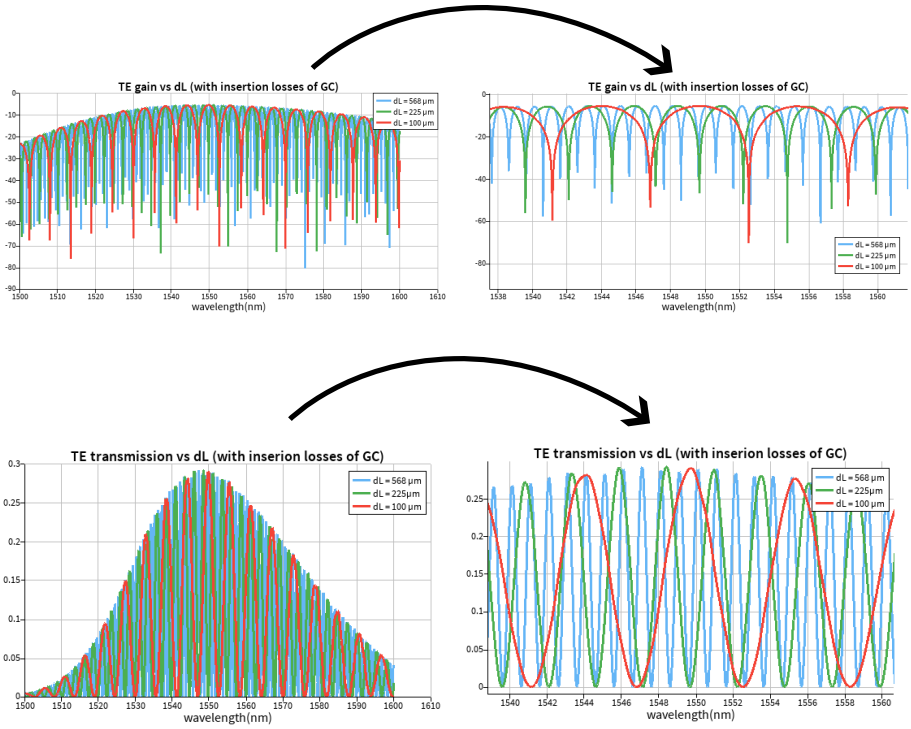

Figure 11. TE gain and transmission data for ΔL = 568 μm, 225 μm and 100 μm including the insertion losses of GC. The right side images are magnified regions.

The FSR is found to decrease(not shown here) with increase in ΔL and for a particular value of $\Delta L = 120 \mu m$, FSR is plotted in Figure 12. The FSR at $\lambda = 1550\ nm$ is 4.9 nm.

4 Michelson Interferometer

Another interferometer of great interest is the Michelson interferometer because the FSR is different from that of MZI due to the inherent path difference the light traverses. Thus, simulations are performed using the layout shown in Figure 13.

ΔL was chosen as 80.6 μm, 243.4 μm and 348.6 μm. The results of data for transmission, TE gain and FSr are shown in Figure 14.

This report is incomplete. I have to submit my PhD thesis this week. So I wish I had the time to work on this report. I really appreciate the effort and the course content. Thank you so much.

5 References

[1] L. Chrostowski and M. Hochberg, “Silicon Photonics Design: From Devices to Systems”, Cambridge University Press, 2015.

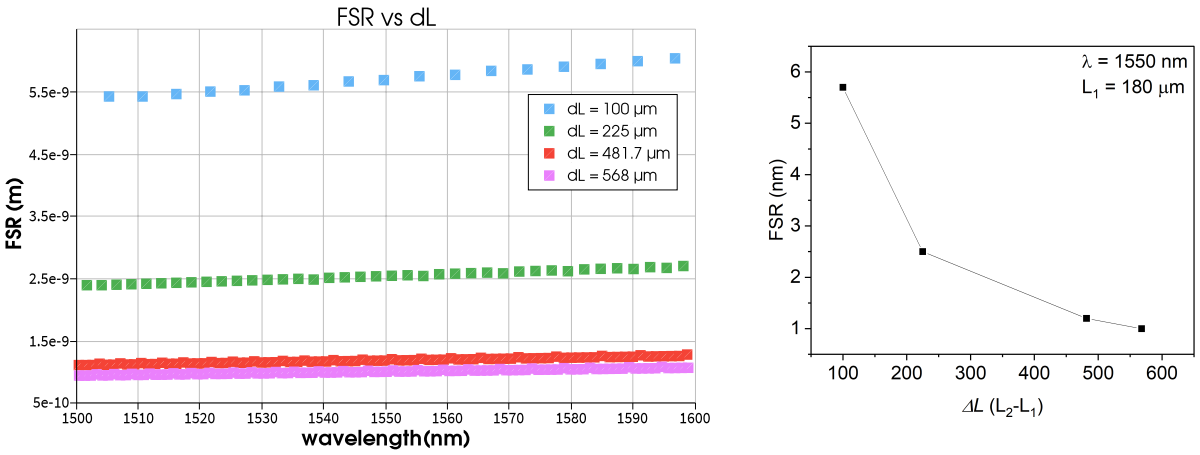

Figure 12. FSR for $L_1 = 180\ \mu m$; and ΔL values of 568 μm, 225 μm and 100 μm. FSR is plotted for $\lambda = 1550\ nm$ for different ΔL values.

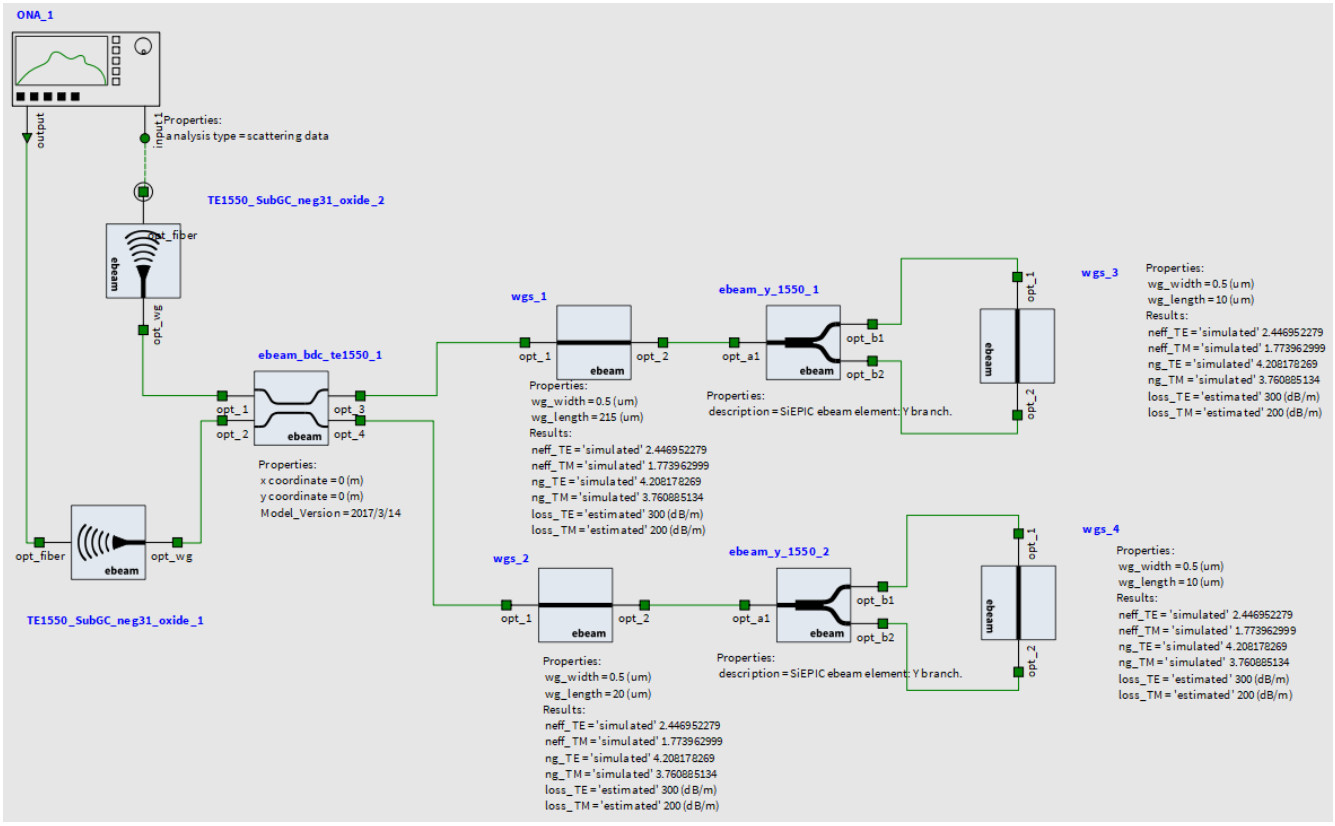

Figure 13. Layout of a Michelson interferometer.

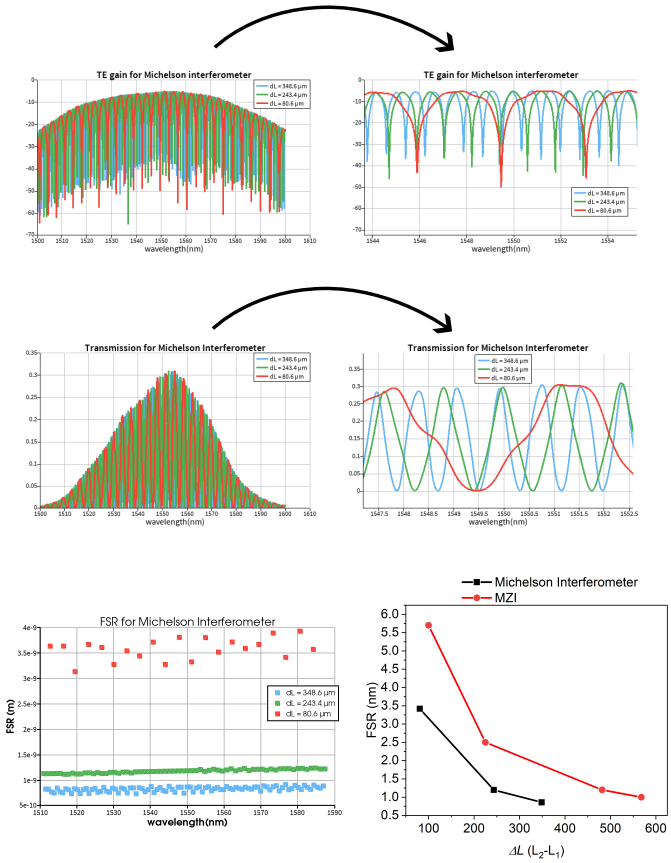

Figure 14. Properties of devices proposed for Michelson Interferometer.

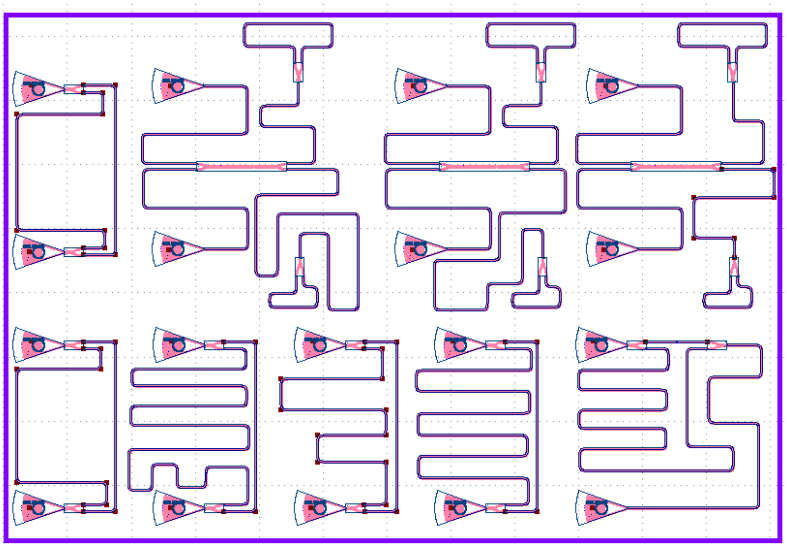

Figure 15. Designs submitted for Fabrication. It includes 6 MZI and 3 Michelson interferometers.